Web based object annotation tool using a Triplet-ReID sorting approach

Afonso Costa[1,2], André L. Ferreira[1,2][a], João M. Fernandes[1][b]
[1] *University of Minho, Braga, Portugal*
[2] *Bosch Car Multimedia Portugal S.A., Braga, Portugal*
{*Afonso.Costa2, Andre.Ferreira2*}*@pt.bosch.com, jmf@di.uminho.pt*

Keywords: Labelling Tool, Triplet Loss, Object Detection, Computer Vision, Deep Learning.

Abstract: The robustness of the object detection methods has seen an increasing attention, which leads to a desire for more control over the training and testing phases. In practice, the need for labelling unique objects present on a dataset can be of help. However, manually labelling datasets of considerable size can be impractical. This paper describes an approach to improve labelling information of a dataset by supporting an object re-identification task. The primary objective is to find repeated objects in the dataset. The proposed solution relies on a web-based application that allows the user to choose which of the similar objects returned by the Triplet-ReID method are in fact the same as the query object. The effectiveness of the method was tested on a dataset with considerable object variability. Experimental results show a viable sorting performance associated with considerable speed improvement when compared to a traditional labelling approach. In fact, a dataset with 55 unique objects in a total of 1098 images would take 18 hours with a traditional tool and 12 hours with proposed one. Moreover, given the generic architecture of the developed framework, it can certainly be applied to a wide range of use cases.

1 INTRODUCTION

Object detection methods have seen substantial improvement over the last few years. In fact, traditional object detection frameworks which were based in handcrafted features and shallow architectures evolved to methods capable of learning high-level feature representation through deeper architectures. Alongside the models, the existing object detection challenges have become more demanding and complex. This change is naturally portrayed in the several competition datasets, such as PASCAL VOC (Everingham et al., 2010) (Everingham et al., 2014), ImageNet (Deng et al., 2010), MS COCO (Lin et al., 2014), and Open Images (Krasin et al., 2017). In detail, the more recent ones tend to have more images, more objects per image and a higher degree of variability in terms of object position, size and placement (Liu et al., 2020). As a result, the newer evaluation process, which belongs to MS COCO, introduced metrics which account for object localization and a more detailed overview of the model's performance using different objects size. As might be expect, all these changes reward models which perform best on all the different scenarios and not just in a particular well-defined use case. Thus, greater importance is being given to the robustness of the proposed models, hence highlighting those that can perform effectively not only in controlled environments, but also in more difficult and diverse real worlds situations.

In order to achieve that goal, it is important to have control over the training and testing phases, specially when it comes to the used objects. In fact, such control enables a better and accurate understanding of the performance during the development of an object detection method. In practice, the need for labelling unique objects in a dataset can be of help in such circumstances. However, when dealing with datasets with considerable size the labelling task can be manually impractical.

The primary objective is to label the objects on a dataset while maintaining trace of their uniqueness, thus enabling finer control over the objects in the train and test sets. For instance, increasing the confidence that the train and test are disjoint sets or excluding objects in certain configurations.

The existing labelling tools are not suited for the use case in question since they all demand the user to transverse every single unlabelled objects each time the labelling occurs for a specific object, which is a

[a] https://orcid.org/0000-0002-7028-426X
[b] https://orcid.org/0000-0003-1174-1966

clearly not optimised workflow that can even make the process unfeasible.

The present work has the goal of developing a new tool that improves such workflow by minimizing the time needed to label the objects of a given dataset. Therefore, this paper contribution consists of a web-based tool which uses the Triplet-ReID deep learning model (Hermans et al., 2017) to sort the unlabelled objects in relation to a query object so that similar ones appear first. Thus, reducing the need to iterate the entire dataset every time.

The applicability of the tool was tested on a real dataset with considerable object variability, both in terms of lighting and perspective. Additionally, a time consumption comparison between the optimised and manual approaches was conducted in order to access the viability of the solution.

The remainder of this paper is organised as follows. Next section gives background and discusses related work. Section 3 presents the architecture, modules and functionality of the developed labelling tool. Section 4 discusses the evaluation process and results. Finally, conclusions are presented in Section 5.

2 BACKGROUND AND RELATED WORK

2.1 Existing labelling tools

There is a high variety of existing labelling tools, for instance, the LabelMe (Russell et al., 2008), Image Labeler App, RectLabel (R. Kawamura, 2020), and LabelImg (Tzutalin,). They all mainly focus on labelling (e.g. segmentation or bounding box annotations) one image at a time. Being the goal to label every object image with a given ID, analysing them repeatedly one by one leads to a cumbersome workflow. Additionally, since the images the not appear in any useful order, the user needs to iterate every single image when labelling each of the existing unique objects.

2.2 Object re-identification

The task of object re-identification (re-ID) can be describe as seeking the occurrences of a query object in a set of candidate objects (gallery). The research in this field has not been very active. In contrast, the person re-identification subtask has attracted increasing attention in recent years mainly due to the automated video surveillance practical applications (Mathur et al., 2020). Naturally, this research area can be seen as a particular use case of the object re-identification task as a whole, thus enabling several solutions to also be used in the later task.

The person re-ID task matches people across a monitoring system of multiple non-overlapping cameras. In practice, given a query image the goal is to found in the gallery those in which the same person appears.

Before 2014, the existing approaches commonly used hand-designed features to represent and match the identity of different objects. The features can be mainly separated in colour based and texture based features, ranging widely from HSV colour histogram (Li and Wang, 2013) (Farenzena et al., 2010), LAB colour histogram (Zhao et al., 2013), SIFT (Zhao et al., 2013), LBP histogram (Li and Wang, 2013), HOG features (Li and Wang, 2013) and Gabor features (Li and Wang, 2013). After the feature extraction process, most models use a simple standard distance measure (e.g. l_1-norm, l_2-norm, Bahattacharyya distance) to evaluate the matching performance between the query and gallery images.

As might be expected, in realistic conditions the person's appearance usually undergoes dramatic visual changes regarding the view angle, resolution, lighting, background clutter and occlusion. Consequently, it becomes challenging to achieve high performance results using handmade feature-based techniques. Additionally, depending on the images conditions, usually there is a subset of features that better represent the identity of the given person. However, the distance measures mentioned above give the same weight to every feature on every use case thus potentially harming the overall method performance. In 2011 papers such as Dikmen *et al.* (Dikmen et al.,) and Zheng *et al.* (Zheng et al., 2011) addressed the aforementioned problems by viewing the person re-identification as a distance learning problem. As a result, the goal shifts from extracting robust appearance features in order to better represent the identity of an individual to learning the optimal distance that maximises the matching accuracy regardless the choice of features. The end goal is to maximise the probability of true matching pairs having a smaller distance than two images of different individuals. Nowadays, this is still an active approach (Hermans et al., 2017) (Wojke and Bewley, 2018) (Yang et al., 2019).

From 2014 onwards, the person re-identification field became increasingly popular and has seen great improvement, mostly due to the deep learning breakthrough. In practice, the methods went from hand-designed features to automatic feature extraction, which opened the field to new possibilities. Yi *et al.*

(Yi et al., 2014) was one of the first papers to apply a deep learning model to the person re-identification problem. The paper proposed a deep metric learning method by using a Siamese convolutional neural network, which allowed the transition from the previously mentioned hand-crafted features and discrete workflow to jointly learning features and metrics in a unified framework.

Currently, most person re-identification models tend to use very specific features such as human body part segmentation (Quan et al., 2019) and spatial-temporal information (Wang et al., 2018) to improvement the models performance. However, these modules make the techniques unsuitable for the object re-identification task in hands, since there is no temporal information and the objects do not always have a human body shape.

3 TOOL

The Figure 1 describes the architecture of the labelling tool. In detail, it encompasses four main components such as the objects dataset, Triplet-ReID module, Flask web framework, and React JavaScript library.

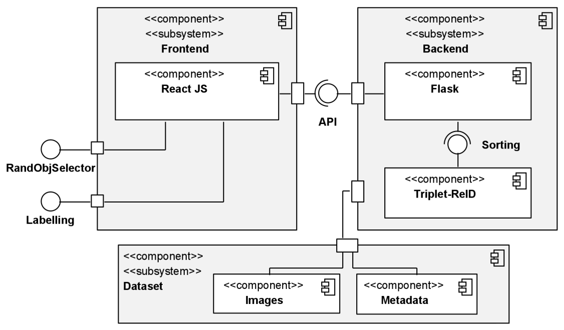

Figure 1: Tool architecture.

Firstly, the objects dataset component represents the directory in which one can find the images as well as the metadata associated to each object. The tool allows one image to have multiple objects. In this case, the metadata must specify each object bounding box, thus enabling their extraction for future processing, for instance by the Triplet-ReID module. All the information needed to represent the dataset can be defined in a configuration file, which decouples the dataset from the actual tool implementation, hence increasing the applicability of the tool.

Secondly, there is the backend which includes the Triplet-ReID python module and Flask. The former is a Triplet-ReID person re-identification model that is imported by Flask and used to sort the results of a given object query. The later is the bridge between all the tool components. Through a REST API, it receives HTTP requests sent by the frontend component and updates its internal state accordingly. In detail, it reads and updates the dataset as the labelling process is fulfilled, while also managing the state of the Triplet-ReID embedding space throughout it's lifespan (initialisation, populate, update, and queries).

Finally, the frontend uses the React JS library in conjunction with the React Bootstrap framework. The later allows for a fast development process since most of the components already exist. Moreover, by using pre-existing components and a minimalist interface the user experience becomes familiar and more fluid.

3.1 Triplet-ReID module

The Triplet-ReID module is used as a sorting algorithm, hence presenting the more similar unlabelled objects first.

The module mainly uses a ResNet-50 architecture with the last layer replaced with two fully connected layers that generate an output of 128 units, which is the final embedding dimension. The training batch encompasses PK images of randomly sampled K instances of randomly sampled P objects. In all experiments, both K and P are set to their default values, 4 and 32 respectively. Afterwards, the batch images are used to generate the training triplets which are a threefold of the current object instance being processed, the hardest positive (more different instance of the same object) and the hardest negative (more similar instance of a different object) within the PK subset. The triplets are then used to compute the Batch Hard loss. As portrayed in the Figure 2, the module uses the Batch Hard loss to project the objects in an embedding space where, eventually, all instances of the same object are closer to each other (lower Euclidean distance) than any instance of a different object (higher Euclidean distance).

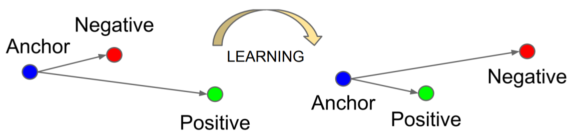

Figure 2: Triplet loss learning workflow. Source: (Schroff et al., 2015)

In practice, in order to sort the unlabelled objects, one needs to project them to the embedding space. Later, an object can be used as query and the module returns the unlabelled objects sorted by similarity.

3.2 Functionality / Workflow

The labelling workflow starts with the random selection of an unlabelled object, in other words, the query object. The random approach allows the user to quickly iterate through the dataset and label an object of their choice. After selecting the object, the remainder of the dataset is sorted with the Triplet-ReID module, hence based on the similarity to the query object. The Figure 3 shows the default view when engaging in the labelling process. In the top of page the user can visualise the query object, alongside some metadata, so it has a reference of the object that its trying to identify. Afterwards, there is two buttons responsible for navigating backward (‘Prev page’) and forward (‘Next page’) in the results list. The third button opens a popup dialog with a list of the selected objects so far, where one can remove an object of the selected list just by clicking on it and finish the labelling process by clicking ‘Save Changes’. Finally, back in the default viewing page one can find the list of proposed unlabelled objects. By default the list presents ten objects at once. The task is to select the images where the query object appears. When doing the selection process the selected objects are replaced by the next object on the list without forcing the user to move to the next page, hence reducing the friction in the process since new objects are automatically appearing on the screen.

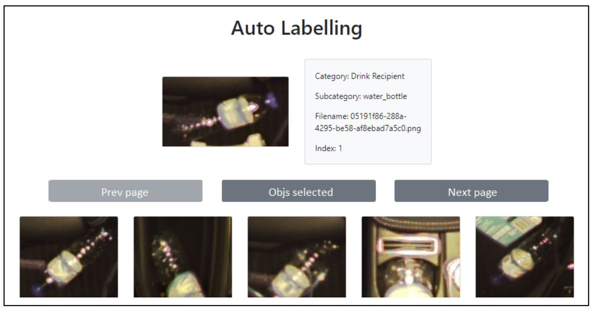

Category: Drink Recipient

Subcategory: water_bottle

Filename: 05191f86-288a-4295-be58-af8ebad7a5c0.png

Index: 1

Figure 3: Layout of the page where the labelling process occurs.

Depending on the object dataset in question, it can be hard to visually understand the object depending on its enviroment (e.g. low light and occlusion). To this end, there is an option to further inspect an object image at any given point. By using the control key and the mouse left click combination, the user has access to the full image where the object is placed. In detail, it is possible to zoom over any specific point of the image. Moreover, it is possible to re-query with an specific object by using the alt key and left mouse click combination. In some specific cases this feature might be useful since re-querying can re-rank the unlabelled objects in a more useful order.

In the end, after having all objects selected the labelling process can actually be completed with the aforementioned ”Save Changes” button, which redirects the user to the random object selection page, restarting the process all over again.

4 EXPERIMENTAL RESULTS

The Table 1 summarises the three datasets, namely A, B and C, used in the experiments with the Triplet-ReID model. All objects were cropped out using their bounding box annotations and none was discarded.

Table 1: Metadata describing the datasets used for training and testing the Triplet-ReID model.

Dataset	Total objs (unique IDs)	Training objs (unique IDs)	Testing objs (unique IDs)
A	2451 (96)	1963 (96)	488 (93)
B	2451 (96)	2231 (83)	220 (13)
C	3684 (145)	2586 (90)	1098 (55)

Firstly, the A and B datasets were generated based on the same collection of objects. The splitting process used to get the train and test sets are the main difference between the two. The former was accomplished by iterating through every object ID and taking 90% of the object instances for training and the remaining 10% for testing. As might be expected, despite having different instances of the same object on the training and testing dataset, the same object appears in both sets, which hinders a proper analyses on the generalisation and robustness of the model. Consequently, in order to evaluate the aforementioned impact, the dataset B uses a default splitting technique, thus splitting the dataset so the set of object IDs in the train and test datasets are disjoint. The C dataset uses the B dataset splitting technique with 70% of the objects going for training and 30% for testing. Furthermore, the C dataset is the union of all the objects present in the B dataset and some novelty ones.

In order to get an accurate understanding of the tool performance, the object instances present in the datasets have high variability, which ultimately increases the difficulty of the sorting task. The Figure 4 shows that variability occurs in terms of size, perspective, light and colour. Furthermore, there are some cases where the object instances are blurry due to low image quality and some are extremely occluded by random components.

Overall, the datasets include objects with high variability obtained in a real world use case, which

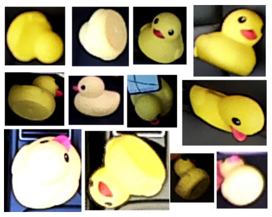
Figure 4: Example of variability within the same object.

allows an evaluation of performance of the labelling tool in a realistic environment.

4.1 Evaluation metrics

The evaluation encompass two different perspectives of the tool: the labelling time and the sorting quality of the unlabelled objects.

On the one hand, the **labelling time** will be evaluated by comparing the same tool with and without the objects sorted by the Triplet-ReID model. Hence, getting a sense of the impact that the sorting can have in the labelling process. In detail, the random approach can be formulated using the following equation:

$$t_r = \sum_{i=0}^{N} (T - M * i) * \alpha \tag{1}$$

where for each N unique objects, the user labels the existing M repetitions by spending α seconds analysing each remaining image in order to decide if it is the query object or not. This process is looped until the user labels all T images in the dataset. It should be highlighted that the equation assumes that all unique objects have the same number of repetitions.

The sorted approach can be approximated by the following equation:

$$t_s = N * (M + E + C) * \alpha \tag{2}$$

where for each N unique objects, the user labels the existing M repetitions by spending α seconds analysing each remaining image in order to decide if it is the query object or not. However, as the model is not capable of placing all matching objects in the first M positions of the results, the E value is the overhead needed to encompass this factor. For instance, if there are 5 matching objects and the overhead is 10, then within the first 15 positions, the user can find the 5 matching results. Additionally, the C constant represents an interval where a matching object does not appear. Normally, this value is equivalent to two pages of objects (20 objects) where no match appears. Afterwards, the formulation assumes that the user saves the existing selected objects and proceeds to the next query.

On the other hand, there is the unlabelled objects **sorting** performance. The Triplet-ReID method proposes a Cumulative Matching Characteristics (CMC) metric (Bolle et al., 2005), which is very popular for person re-identification methods. However, the aforementioned metric does not portrait well the sorting performance since the goal is not to evaluate how soon a correct object appears in the ranking but how much are placed in the early positions of the ranking.

In order to solve the previous issue, the CMC metric was replaced to encompass the new perspective in which the model is being used. To this end, three new metrics were introduced: mean average precision (mAP), Rank-K accuracy and average distance (AD).

Firstly, the area under the Precision-Recall curve is used to compute the average precision (AP) of each querying object. Afterwards, the mean of all AP values produces the mAP metric. (Zheng et al., 2015)

In practice, a lower mAP value means that the user needs to cycle through more objects than it needs to label all instances of an object. In contrast, a perfect mAP would mean that the user only needs to iterate the exact number of correct objects to label them all.

Secondly, the Rank-K accuracy is the result of averaging the division of the correct objects (c) by the first K positions of the sorted objects. Therefore, the Rank-K accuracy metric can be summarised as:

$$\text{Rank-K accuracy} = \frac{\sum_{i=1}^{N} \frac{c}{K}}{N} \tag{3}$$

For instance, if one is trying to label an object with 100 unlabelled instances, a lower Rank-100 accuracy means that a low number of those instances are within the first 100 positions. In contrast, a higher Rank-100 accuracy portraits a sorting order where a higher number of correct objects are within the first 100 positions.

Lastly, there is the AD which directly portraits the average distance between the correct objects positions after being sorted. For instance, a AD of 2.5 for a given query object means that the unlabelled instances of such object have an average distance of 2.5 objects between them. In other words, a lower AD results in correct objects being closer to one another and a higher AD the opposite. Ideally, one wants an AD below two pages of objects so that correct objects are continuously seen throughout the labelling, which results in a more fluid experience.

4.2 Results

Analysing the time consumption metrics in a more practical point of view, the random approach (Eq. 1) enforces the user to transverse every remaining object

Table 2: Experiments with A dataset.

Experiment name	mAP (%)	Rank-K accuracy (%)	AD (objects)	Train augmentation	Embedding augmentation	Net	Head
EA3	88.77	84.52	1.5784	flip	-	ResNet50 v1 (pre-trained on ImageNet)	Fully connected (1024x1024)
EA5	88.91	84.20	2.5468	flip+crop	-		
EA6	88.36	84.25	2.3895	-	flip		
EA7	90.78	88.05	3.1601	-	crop		
EA9	86.78	81.83	1.8556	flip	flip		
EA12	89.51	85.72	2.3761	flip+crop	flip+crop		
EA15	88.38	84.74	3.1141	flip+crop	flip+crop	ResNet101 v1 (pre-trained on ImageNet)	
EA16	90.95	88	1.8446	flip	flip		

Table 3: Experiments with B dataset.

Experiment name	mAP (%)	Rank-K accuracy (%)	AD (objects)	Train augmentation	Embedding augmentation	Net	Head
EB3	82.52	76.52	5.9809	flip	-	ResNet50 v1 (pre-trained on ImageNet)	Fully connected (1024x1024)
EB5	79.26	73.01	5.4948	flip+crop	-		
EB6	81.94	75.92	4.5859	-	flip		
EB7	86.08	80.86	4.3681	-	crop		
EB9	79.75	73.60	6.0326	flip	flip		
EB12	78.00	71.90	5.2936	flip+crop	flip+crop		
EB15	79.04	72.67	5.8664	flip+crop	flip+crop	ResNet101 v1 (pre-trained on ImageNet)	
EB16	82.11	75.37	4.9387	flip	flip		

image for each query object. In contrast, the sorted version (Eq. 2) puts the control on the user so he can stop earlier. Consequently, depending on the dataset one approach can be better than the other. Therefore, if the dataset has few unique objects (N) but each with a high number of repetitions than the random approach can actually be better. Whereas, if the dataset has a higher number of unique objects and each with a low number of repetitions than the sorted version can achieve better results, hence a faster labelling process.

An analyses was performed by using fictitious datasets FB and FC which are lightly based on the B and C dataset, respectively. The FB dataset can be describe with the following values: $T = 220$, $N = 13$, $M = 16$, $C = 20$, $E = 32$, and $\alpha = 2$. Similarly, the FC dataset is defined by the following constants: $T = 1098$, $N = 55$, $M = 19$, $C = 20$, $E = 357$, and α = 2.

When using the FB dataset, the random approach (t_r) would take about 54 minutes to complete the labelling. Meanwhile, the sorted approach (t_s) would take only about 30 minutes. Furthermore, when simulating with a bigger dataset such as the FC the t_r time increases significantly reaching the 18 hours while the t_s time would stay at about 12 hours. Naturally, bigger datasets yield larger differences, making the random approach quickly unfeasible in a business context.

Regarding the Triplet-ReID module, the same experiments were performed with each of the three previously mentioned datasets. In detail, each experiment started by training the model with the appropriate images of each dataset on a set of parameters, such as the network architecture, the use of pre-trained weights and crop/flip augmentations. The rest of the parameters remained with their default values as changing them did not improved the model performance. Next, the trained model is used to project the test images to an embedding space. As in training, the embedding stage enables crop and flip augmentations as well. Lastly, the evaluation phase computes the mAP, Rank-K accuracy and AD metrics by querying all the test images over the populated embedding space.

The Table 2 shows the results yield by the A dataset. The highest performance increase is due to the use of the pretrained weights. In contrast, there is no meaningful performance difference between the experiments done with the `resnet_v1_50` and the `resnet_v1_101` networks. The best results were achieved with the EA7 experiment with a mAP of 90.78%, Rank-K accuracy of 88.05% and AD of 3.1601, and the EA16 experiment with a mAP of 90.95%, Rank-K accuracy of 88% and an AD of 1,8446.

The same experiments were conducted using the B dataset and the results are reported in Table 3. The best results were achieved in the EB3 and EB7 experiments. The main difference between the EB and EA set of experiments is the splitting algorithm used to separate the training and testing data. As might be expected, all metrics decreased. The main reason is the novelty of the testing objects used as the model had never seen them. The 7.97% decrease in mAP, 10.18% decrease in Rank-K accuracy and the increase of 2.9620 objects in the AD metric show that the correct objects are further away from the first positions

Table 4: Experiments with C dataset.

Experiment name	mAP (%)	Rank-K accuracy (%)	AD (objects)	Train augmentation	Embedding augmentation	Net	Head
EC3	45.01	43.07	20.1552	flip	-	ResNet50 v1 (pre-trained on ImageNet)	Fully connected (1024x1024)
EC5	44.62	42.57	20.7063	flip+crop	-		
EC6	49.27	45.91	16.855	-	flip		
EC7	45.81	43.54	21.3495	-	crop		
EC9	48.66	45.79	17.9821	flip	flip		
EC12	46.50	44.06	20.072	flip+crop	flip+crop		
EC15	47.01	44.36	19.4776	flip+crop	flip+crop	ResNet101 v1 (pre-trained on ImageNet)	
EC16	50.82	47.47	15.7853	flip	flip		

as well as more distant from each other.

The results of the experiments with the C dataset are reported in the Table 4. The main difference is the significant lower metric values, with a decrease of 33.88% in mAP, 30.39% in Rank-K accuracy, and an increase of 13.7278 objects in AD. Despite, the goal of generating a more discriminative model through using more training samples, the performance impact suggests that the new objects added to the C dataset are in fact harder to distinguish, thus resulting in lower metrics overall.

Lastly, after querying the system with a variety of objects, one can notice a pattern regarding the real size of the objects. In fact, all objects are cropped by their bounding box and resized to height of 256 pixels and a width of 128 pixels. Consequently, it becomes impossible to compare their actual size since objects with major size differences can fill the same percentage of the final image. As a result, objects which have a similar appearance but a noticeable size difference are usually challenging for the system to distinguish. Figure 5 shows some practical examples were the problem appears.

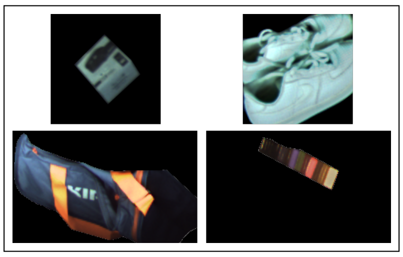

Figure 5: Examples were the size problem is evident. The first column shows a query object and the second column shows an object that appears within the first 10 positions of the results.

5 CONCLUSION

Due to the importance of the robustness in object detection models, having control over the objects in both the training and testing phase is crucial. The identification of all unique objects using existing labelling tools becomes an inefficient workflow since they only allow the analyses of one image at once, which could even make the labelling process unfeasible in large datasets.

This paper proposes a web based tool coupled with the Triplet-ReID model to improve the labelling process. The addition of the machine learning module allows the sorting of unlabelled objects by similarity. Furthermore, being a web-based application enables its deployment locally or on external servers, hence allowing for both private and crowdsourced labelling strategies.

The experiments demonstrate the viability of the solution both in terms of sorting performance and labelling time when compared to a random approach, specially when using a dataset of with high number of different objects and each with a low number of repetitions. Moreover, given the generic architecture of the developed framework, it can certainly be applied to a wide range of use cases.

As future work, the experiments should be replicated with larger datasets as the size of the ones used can influence the reported results. Also, the addition of visual attention learning mechanism to re-weight the learned feature maps will be explored to access their impact on the objects similarity sorting performance (Li et al., 2018) (Song et al., 2018) (Si et al., 2018) (Chen et al., 2020). Moreover, several techniques to maintain the scale between objects will be experimented in order to make their size a valuable feature on the object re-identification task.

ACKNOWLEDGEMENTS

This work is supported by: European Structural and Investment Funds in the FEDER component, through the Operational Competitiveness and Internationalization Programme (COMPETE 2020) [Project nº 039334; Funding Reference: POCI-01-0247-FEDER-039334]

REFERENCES

Bolle, R. M., Connell, J. H., Pankanti, S., Ratha, N. K., and Senior, A. W. (2005). The Relation Between the ROC Curve and the CMC. Technical report.

Chen, Y., Wang, H., Sun, X., Fan, B., and Tang, C. (2020). Deep Attention Aware Feature Learning for Person Re-Identification.

Deng, J., Dong, W., Socher, R., Li, L.-J., Kai Li, and Li Fei-Fei (2010). ImageNet: A large-scale hierarchical image database. pages 248–255. Institute of Electrical and Electronics Engineers (IEEE).

Dikmen, M., Akbas, E., Huang, T. S., and Ahuja, N. Pedestrian Recognition with a Learned Metric. Technical report.

Everingham, M., Eslami, S. M., Van Gool, L., Williams, C. K., Winn, J., and Zisserman, A. (2014). The Pascal Visual Object Classes Challenge: A Retrospective. *International Journal of Computer Vision*, 111(1):98–136.

Everingham, M., Van Gool, L., Williams, C. K., Winn, J., and Zisserman, A. (2010). The pascal visual object classes (VOC) challenge. *International Journal of Computer Vision*, 88(2):303–338.

Farenzena, M., Bazzani, L., Perina, A., Murino, V., and Cristani, M. (2010). Person re-identification by symmetry-driven accumulation of local features. In *Proceedings of the IEEE Computer Society Conference on Computer Vision and Pattern Recognition*, pages 2360–2367.

Hermans, A., Beyer, L., and Leibe, B. (2017). In Defense of the Triplet Loss for Person Re-Identification.

Krasin, I., Duerig, T., Alldrin, N., Ferrari, V., Abu-El-Haija, S., Kuznetsova, A., Rom, H., Uijlings, J., Popov, S., Kamali, S., Malloci, M., Pont-Tuset, J., Veit, A., Belongie, S., Gomes, V., Gupta, A., Sun, C., Chechik, G., Cai, D., Feng, Z., Narayanan, D., and Murphy, K. (2017). OpenImages: A public dataset for large-scale multi-label and multi-class image classification. *Dataset available from https://storage.googleapis.com/openimages/web/index.html*.

Li, W. and Wang, X. (2013). Locally aligned feature transforms across views. In *Proceedings of the IEEE Computer Society Conference on Computer Vision and Pattern Recognition*, pages 3594–3601.

Li, W., Zhu, X., and Gong, S. (2018). Harmonious Attention Network for Person Re-Identification.

Lin, T.-Y., Maire, M., Belongie, S., Bourdev, L., Girshick, R., Hays, J., Perona, P., Ramanan, D., Zitnick, C. L., and Dollár, P. (2014). Microsoft COCO: Common Objects in Context.

Liu, L., Ouyang, W., Wang, X., Fieguth, P., Chen, J., Liu, X., and Pietikäinen, M. (2020). Deep Learning for Generic Object Detection: A Survey. *International Journal of Computer Vision*, 128(2):261–318.

Mathur, N., Mathur, S., Mathur, D., and Dadheech, P. (2020). A Brief Survey of Deep Learning Techniques for Person Re-identification. In *Proceedings of 3rd International Conference on Emerging Technologies in Computer Engineering: Machine Learning and Internet of Things, ICETCE 2020*, pages 129–138. Institute of Electrical and Electronics Engineers Inc.

Quan, R., Dong, X., Wu, Y., Zhu, L., and Yang, Y. (2019). Auto-ReID: Searching for a Part-aware ConvNet for Person Re-Identification.

R. Kawamura (2020). RectLabel.

Russell, B. C., Torralba, A., Murphy, K. P., and Freeman, W. T. (2008). LabelMe: A database and web-based tool for image annotation. *International Journal of Computer Vision*, 77(1-3):157–173.

Schroff, F., Kalenichenko, D., and Philbin, J. (2015). FaceNet: A Unified Embedding for Face Recognition and Clustering.

Si, J., Zhang, H., Li, C. G., Kuen, J., Kong, X., Kot, A. C., and Wang, G. (2018). Dual Attention Matching Network for Context-Aware Feature Sequence Based Person Re-identification. In *Proceedings of the IEEE Computer Society Conference on Computer Vision and Pattern Recognition*, pages 5363–5372. IEEE Computer Society.

Song, C., Huang, Y., Ouyang, W., and Wang, L. (2018). Mask-Guided Contrastive Attention Model for Person Re-identification. In *Proceedings of the IEEE Computer Society Conference on Computer Vision and Pattern Recognition*, pages 1179–1188. IEEE Computer Society.

Tzutalin. LabelImg.

Wang, G., Lai, J., Huang, P., and Xie, X. (2018). Spatial-Temporal Person Re-identification.

Wojke, N. and Bewley, A. (2018). Deep Cosine Metric Learning for Person Re-Identification.

Yang, X., Wang, M., and Tao, D. (2019). Person Re-identification with Metric Learning using Privileged Information.

Yi, D., Lei, Z., and Li, S. Z. (2014). Deep Metric Learning for Practical Person Re-Identification.

Zhao, R., Ouyang, W., and Wang, X. (2013). Unsupervised salience learning for person re-identification. In *Proceedings of the IEEE Computer Society Conference on Computer Vision and Pattern Recognition*, pages 3586–3593.

Zheng, L., Shen, L., Tian, L., Wang, S., Wang, J., and Tian, Q. (2015). Scalable Person Re-identification: A Benchmark. In *2015 IEEE International Conference on Computer Vision (ICCV)*, pages 1116–1124. IEEE.

Zheng, W. S., Gong, S., and Xiang, T. (2011). Person re-identification by probabilistic relative distance comparison. In *Proceedings of the IEEE Computer Society Conference on Computer Vision and Pattern Recognition*, pages 649–656. IEEE Computer Society.